Supplemental material for:

FtsA regulates Z-ring morphology and cell wall metabolism in an FtsZ C-terminal linker dependent manner in *C. crescentus*

Jordan M. Barrows*, Kousik Sundararajan*#, Anant Bhargava, and Erin D. Goley

Department of Biological Chemistry, Johns Hopkins University School of Medicine, Baltimore, MD 21205

* These authors contributed equally to this work.

Current affiliation: Department of Biochemistry, Stanford University, Stanford, CA 94305

Supplemental references:

1. Goley ED, Dye NA, Werner JN, Gitai Z, Shapiro L. 2010. Imaging-Based Identification of a Critical Regulator of FtsZ Protofilament Curvature in *Caulobacter*. Molecular Cell 39:975–987.

2. Sundararajan K, Miguel A, Desmarais SM, Meier EL, Huang KC, Goley ED. 2015. The bacterial tubulin FtsZ requires its intrinsically disordered linker to direct robust cell wall construction. Nature Communications 1–14.

3. Woldemeskel SA, McQuillen R, Hessel AM, Xiao J, Goley ED. 2017. A conserved coiled-coil protein pair focuses the cytokinetic Z-ring in *Caulobacter crescentus*. Molecular Microbiology 105:721–740.

4. Ohta N, Ninfa AJ, Allaire A, Kulick L, Newton A. 1997. Identification, characterization, and chromosomal organization of cell division cycle genes in *Caulobacter crescentus*. Journal of Bacteriology 179:2169–2180.

5. Meier EL, Razavi S, Inoue T, Goley ED. 2016. A novel membrane anchor for FtsZ is linked to cell wall hydrolysis in *Caulobacter crescentus*. Molecular Microbiology 101:265–280.

6. Meier EL, Daitch AK, Yao Q, Bhargava A, Jensen GJ, Goley ED. 2017. FtsEX-mediated regulation of the final stages of cell division reveals morphogenetic plasticity in *Caulobacter crescentus*. PLoS Genet 13:e1006999.

7. Thanbichler M, Iniesta AA, Shapiro L. 2007. A comprehensive set of plasmids for vanillate- and xylose-inducible gene expression in *Caulobacter crescentus*. Nucleic Acids Res 35:e137.

8. Evinger M, Agabian N. 1977. Envelope-associated nucleoid from *Caulobacter crescentus* stalked and swarmer cells. Journal of Bacteriology 132:294–301.

9. Goley ED, Yeh Y-C, Hong S-H, Fero MJ, Abeliuk E, McAdams HH, Shapiro L. 2011. Assembly of the *Caulobacter* cell division machine. Molecular Microbiology 80:1680–1698.

10. Thanbichler M, Shapiro L. 2006. MipZ, a spatial regulator coordinating chromosome segregation with cell division in *Caulobacter*. Cell 126:147–162.

11. Du S, Park KT, Lutkenhaus J. 2015. Oligomerization of FtsZ converts the FtsZ tail motif (conserved carboxy-terminal peptide) into a multivalent ligand with high avidity for partners ZipA and SlmA. Molecular Microbiology 95:173–188.

12. The PyMOL Molecular Graphics System, Version 2.0, Schrödinger, LLC.

Supplemental figures:

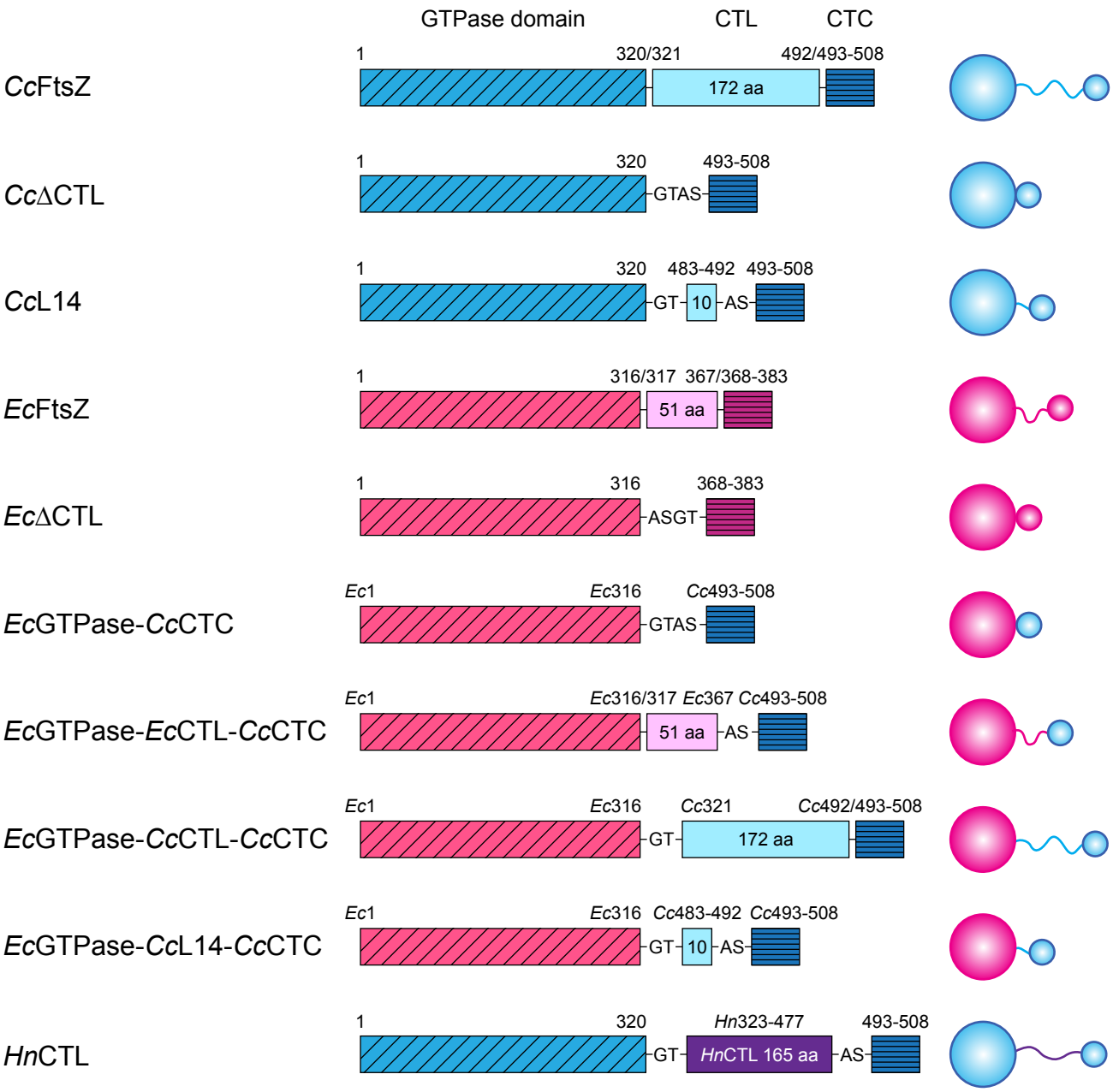
GTPase domain
CTL
CTC
CcFtsZ
1
320/321
492/493-508
172 aa
CcΔCTL
1
320
493-508
GTAS
CcL14
1
320
483-492
493-508
GT
10
AS
EcFtsZ
1
316/317
367/368-383
51 aa
EcΔCTL
1
316
368-383
ASGT
EcGTPase-CcCTC
Ec1
Ec316
Cc493-508
GTAS
EcGTPase-EcCTL-CcCTC
Ec1
Ec316/317
Ec367
Cc493-508
51 aa
AS
EcGTPase-CcCTL-CcCTC
Ec1
Ec316
Cc321
Cc492/493-508
GT
172 aa
EcGTPase-CcL14-CcCTC
Ec1
Ec316
Cc483-492
Cc493-508
GT
10
AS
HnCTL
1
320
Hn323-477
493-508
GT
HnCTL 165 aa
AS

Figure S1

Figure S1: Domain architecture of FtsZ CTL variants

Domain structures of *Cc*FtsZ, *Cc*ΔCTL, *Cc*L14, *Ec*FtsZ, *Ec*ΔCTL, *Cc/Ec* chimeras, and *Hn*CTL FtsZ variants used in this study. Residue numbers are indicated.

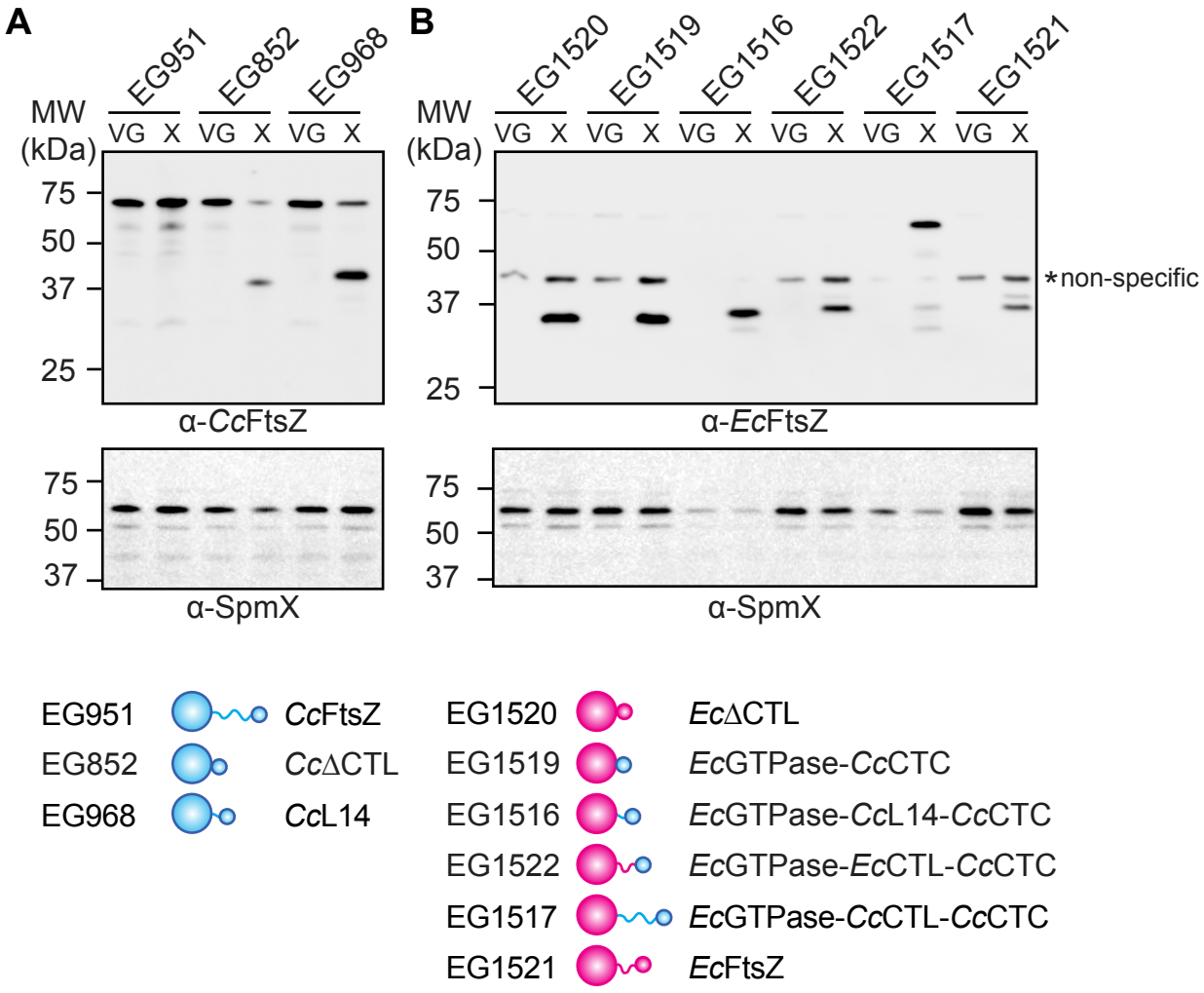
A
EG951
EG852
EG968
MW (kDa)
VG X VG X VG X
75
50
37
25
α-CcFtsZ
75
50
37
α-SpmX
B
EG1520
EG1519
EG1516
EG1522
EG1517
EG1521
MW (kDa)
VG X VG X VG X VG X VG X VG X
75
50
37
25
*non-specific
α-EcFtsZ
75
50
37
α-SpmX
EG951 CcFtsZ
EG852 CcΔCTL
EG968 CcL14
EG1520 EcΔCTL
EG1519 EcGTPase-CcCTC
EG1516 EcGTPase-CcL14-CcCTC
EG1522 EcGTPase-EcCTL-CcCTC
EG1517 EcGTPase-CcCTL-CcCTC
EG1521 EcFtsZ

Figure S2

Figure S2: FtsZ chimeras are produced to similar steady state levels.

A.-B. Immunoblots using anti-*Cc*FtsZ (**A**) and anti-*Ec*FtsZ (**B**) antibodies showing levels of chimeric FtsZ variants shown in Figure 1A. SpmX was used as a loading control. VG – vanillate+glucose control with only WT Cc*FtsZ* expression. X – xylose driven expression of FtsZ chimeras for 5 hours. Anti-SpmX antibody was used as concentration control for loading. Strain key: *Cc*FtsZ (EG951), *Cc*ΔCTL (EG852), *Cc*L14 (EG968), *Ec*FtsZ (EG1521), *Ec*ΔCTL (EG1520), *Ec*GTPase-*Cc*CTC (EG1519), *Ec*GTPase-*Ec*CTL-*Cc*CTC (EG1522), *Ec*GTPase-*Cc*CTL-*Cc*CTC (EG1517), *Ec*GTPase-*Cc*L14-*Cc*CTC (EG1516)

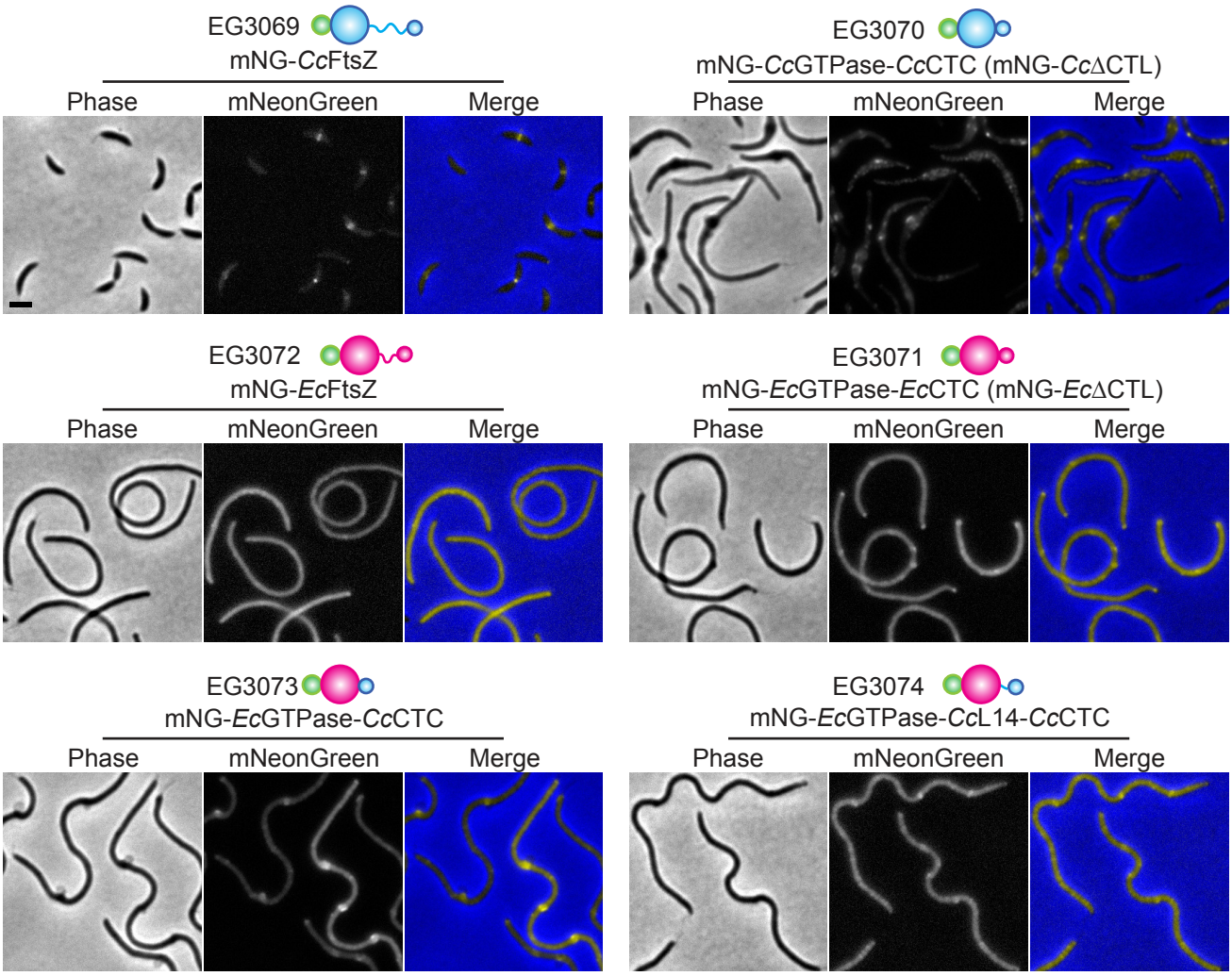
EG3069
mNG-CcFtsZ
Phase
mNeonGreen
Merge
EG3070
mNG-CcGTPase-CcCTC (mNG-CcΔCTL)
Phase
mNeonGreen
Merge
EG3072
mNG-EcFtsZ
Phase
mNeonGreen
Merge
EG3071
mNG-EcGTPase-EcCTC (mNG-EcΔCTL)
Phase
mNeonGreen
Merge
EG3073
mNG-EcGTPase-CcCTC
Phase
mNeonGreen
Merge
EG3074
mNG-EcGTPase-CcL14-CcCTC
Phase
mNeonGreen
Merge

Figure S3

Figure S3: The *E. coli* GTPase domain is unable to localize properly when produced in *C. crescentus*.

Phase contrast, epifluorescence, and merged images of cells induced with xylose to drive production of indicated mNeonGreen (green) fusions to *C. crescentus* FtsZ (cyan), *E. coli* FtsZ (magenta), CTL truncations, or their chimeric variants from P_{xylX} for 5 hours prior to imaging. Scale bar – 2 µm. Strain key: mNG-*Cc*FtsZ (EG3069), mNG-*Cc*ΔCTL (EG3070), mNG-*Ec*FtsZ (EG3072), mNG-*Ec*ΔCTL (EG3071), mNG-*Ec*GTPase-*Cc*CTC (EG3073), mNG-*Ec*GTPase-*Cc*L14-*Cc*CTC (EG3074)

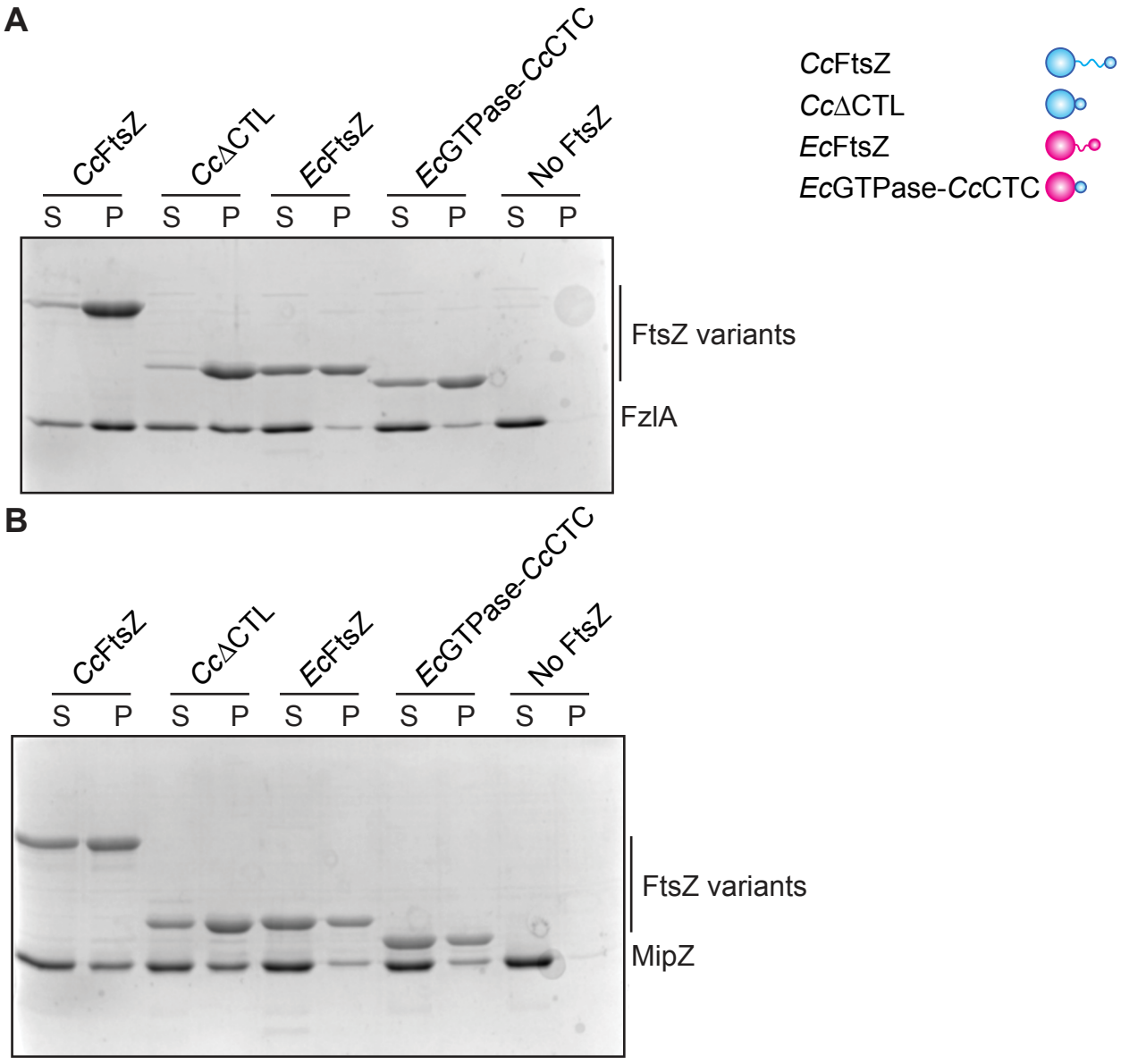
A
CcFtsZ
CcΔCTL
EcFtsZ
EcGTPase-CcCTC
No FtsZ
S P S P S P S P S P
FtsZ variants
FzlA
CcFtsZ
CcΔCTL
EcFtsZ
EcGTPase-CcCTC
B
CcFtsZ
CcΔCTL
EcFtsZ
EcGTPase-CcCTC
No FtsZ
S P S P S P S P S P
FtsZ variants
MipZ

Figure S4

Figure S4: FzlA and MipZ do not bind efficiently to the GTPase domain of *E. coli* FtsZ.

A.-B. Coomassie-stained SDS-PAGE of supernatant (S) and pellet (P) after high-speed centrifugation of 5 µM FzlA (**A**) or MipZ (**B**) with 5 µM *Cc*FtsZ, *Cc*ΔCTL, *Ec*FtsZ, *Ec*GTPase-*Cc*CTC, or no FtsZ variant incubated in HEK50 buffer with 10 mM $MgCl_2$, 2 mM GTP, 0.05% Triton X-100, and, for B., 2 mM ATP.

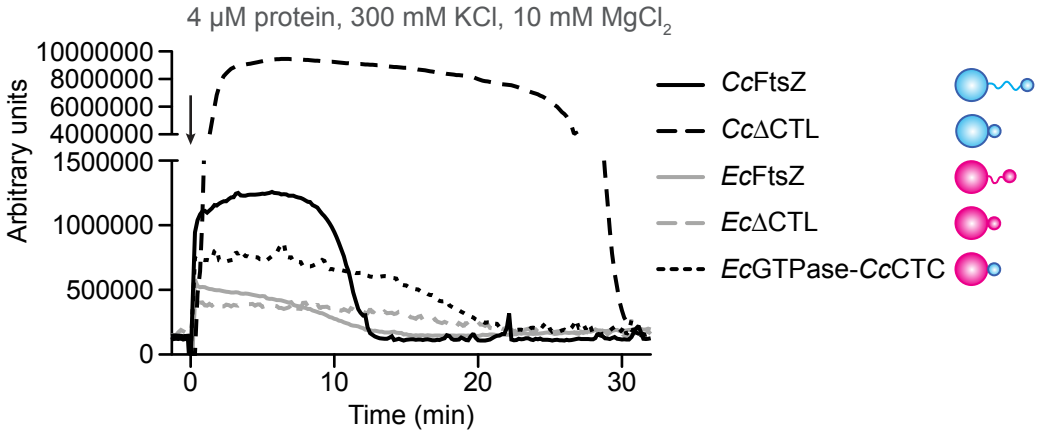
4 µM protein, 300 mM KCl, 10 mM MgCl2
Arbitrary units
10000000
8000000
6000000
4000000
1500000
1000000
500000
0
0
10
20
30
Time (min)
CcFtsZ
CcΔCTL
EcFtsZ
EcΔCTL
EcGTPase-CcCTC

Figure S5

Figure S5: *C. crescentus* and *E. coli* ΔCTL variants exhibit increased stability compared to their respective FtsZs

Right angle light scatter at 350 nm over time for 4 μM FtsZ variants incubated in HEK300 buffer with 10 mM $MgCl_2$ and 0.5 mM GTP (added at time $t = 0$ min; black arrow). Representative curves of three independent replicates are shown for each variant.

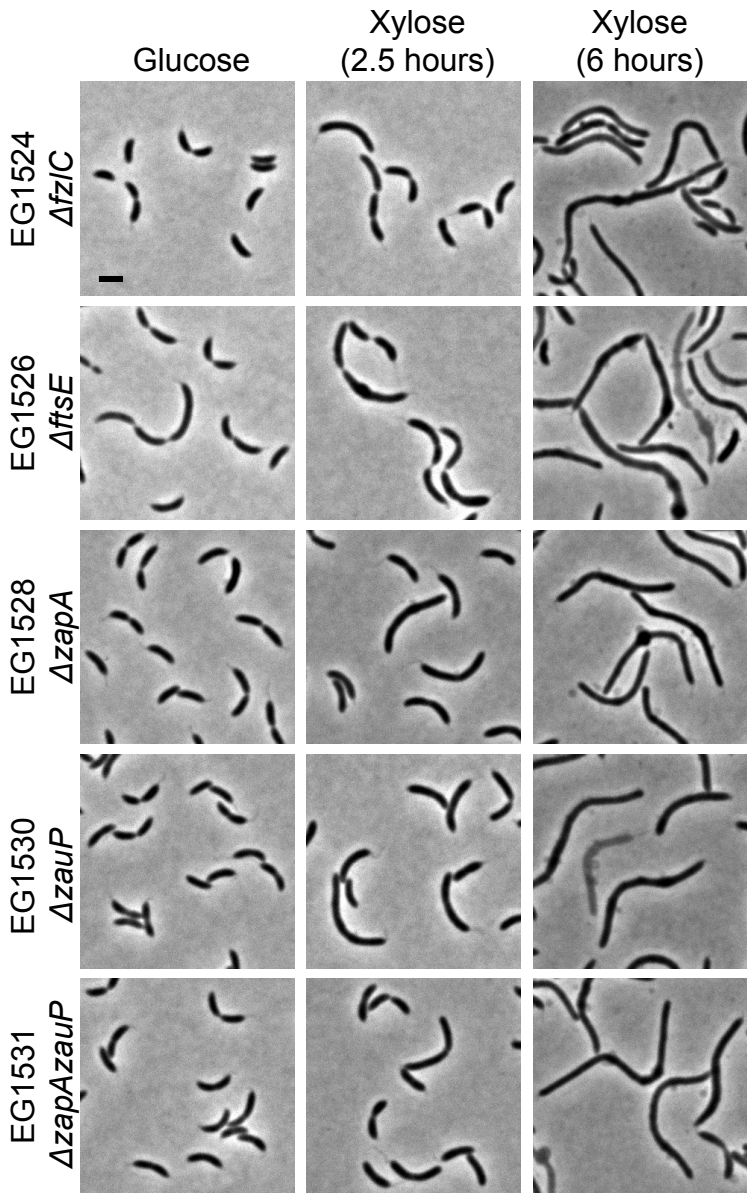
Glucose
Xylose
(2.5 hours)
Xylose
(6 hours)
EG1524
ΔftsIC
EG1526
ΔftsE
EG1528
ΔzapA
EG1530
ΔzauP
EG1531
ΔzapAzauP

Figure S6

Figure S6: Non-essential FtsZ-binding partners are not required for ΔCTL-induced bulges.

Phase contrast images showing the morphologies of cells in the absence and presence of inducer (xylose) for expression of Δ*CTL* in strains deleted for the non-essential binding partners of FtsZ. Scale bar – 2 μm. Strain key (all have xylose-inducible Δ*CTL*): Δ*fzlC* (EG1524), Δ*ftsE* (EG1526), Δ*zapA* (EG1528), Δ*zauP* (EG1530), Δ*zapAzauP* (EG1531)

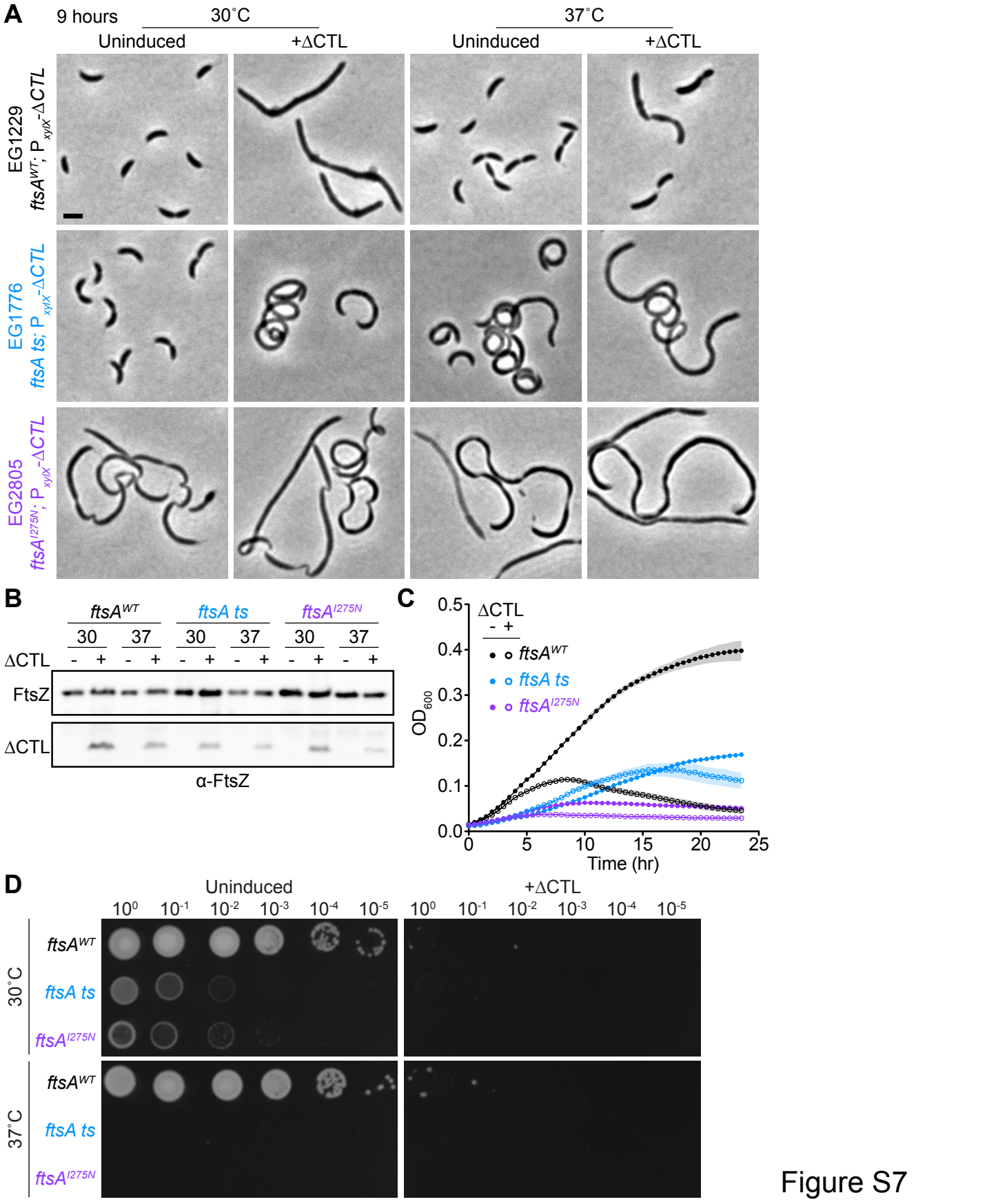
A
9 hours
30˚C
37˚C
Uninduced
+ΔCTL
Uninduced
+ΔCTL
EG1229
ftsA^WT; P_xylX-ΔCTL
EG1776
ftsA ts; P_xylX-ΔCTL
EG2805
ftsA^I275N; P_xylX-ΔCTL
B
ftsA^WT
ftsA ts
ftsA^I275N
30
37
30
37
30
37
ΔCTL
- + - + - + - + - + - +
FtsZ
ΔCTL
α-FtsZ
C
ΔCTL
- +
ftsA^WT
ftsA ts
ftsA^I275N
OD600
0.5
0.4
0.3
0.2
0.1
0.0
0
5
10
15
20
25
Time (hr)
D
Uninduced
+ΔCTL
10^0 10^-1 10^-2 10^-3 10^-4 10^-5 10^0 10^-1 10^-2 10^-3 10^-4 10^-5
30˚C
37˚C
ftsA^WT
ftsA ts
ftsA^I275N
ftsA^WT
ftsA ts
ftsA^I275N

Figure S7

Figure S7: A temperature sensitive *ftsA* mutant suppresses formation of ΔCTL-induced bulges.

A. Phase contrast images of cells with WT *ftsA* or a temperature sensitive allele of *ftsA* in its original mutagenized background (*ftsA ts*) or in an otherwise wild type background ($ftsA^{I275N}$) uninduced with glucose or induced with xylose (+ΔCTL) for Δ*CTL* expression at 30˚C or 37˚C for 9 hours prior to imaging. Scale bar – 2 μm. **B.** Immunoblot using anti-FtsZ antibody on lysates from strains from A. uninduced with glucose (-ΔCTL) or induced with xylose (+ΔCTL) for Δ*CTL* expression at 30˚C or 37˚C for 9 hours. **C.** Growth characteristics of the strains from A. uninduced (closed circles) or induced (open circles) for Δ*CTL* expression and grown for 24 hours at 30˚C. Shaded regions represent SD of three technical replicates at each point. **D.** Spot dilutions of strains from A. Cells in log phase were diluted to an OD_{600} of 0.05, serially diluted, and spotted onto PYE agar plates with either glucose (uninduced) or xylose (+ΔCTL). Plates were incubated at 30˚C for 48 hours before imaging. Strain key (all have xylose-inducible Δ*CTL*): $ftsA^{WT}$ (EG1229), *ftsA ts* (EG1776), $ftsA^{I275N}$ (EG2805)

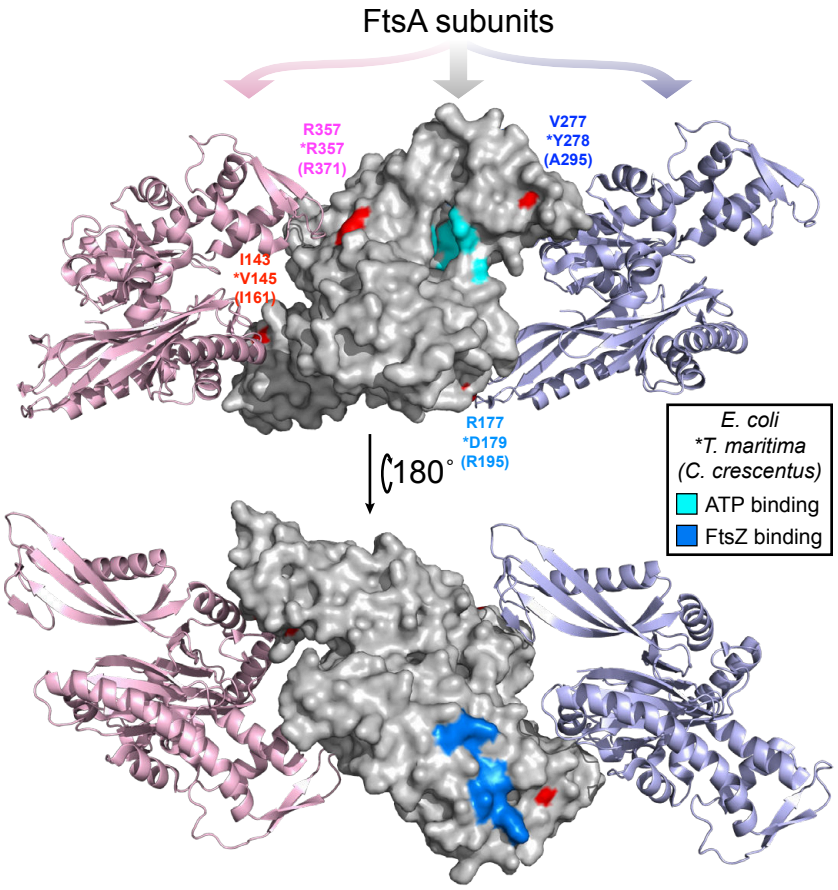

Adapted from PDB: 4A2B

Figure S8

Figure S8: Locations of *ftsA* point mutations proposed to disrupt self-interaction.

Each of the four analogous residues proposed to disrupt FtsA self-interaction (red) mapped onto a surface rendering (grey) of *T. maritima* FtsA in complex with two other FtsA monomers (cartoon, pink and lilac). Analogous residues in *E. coli*, *T. maritima*, and *C. crescentus* are indicated next to each location. The ATP- and FtsZ-binding sites are indicated in cyan and blue, respectively. Model was constructed using PDB: 4A2B in the PyMOL (12) program.

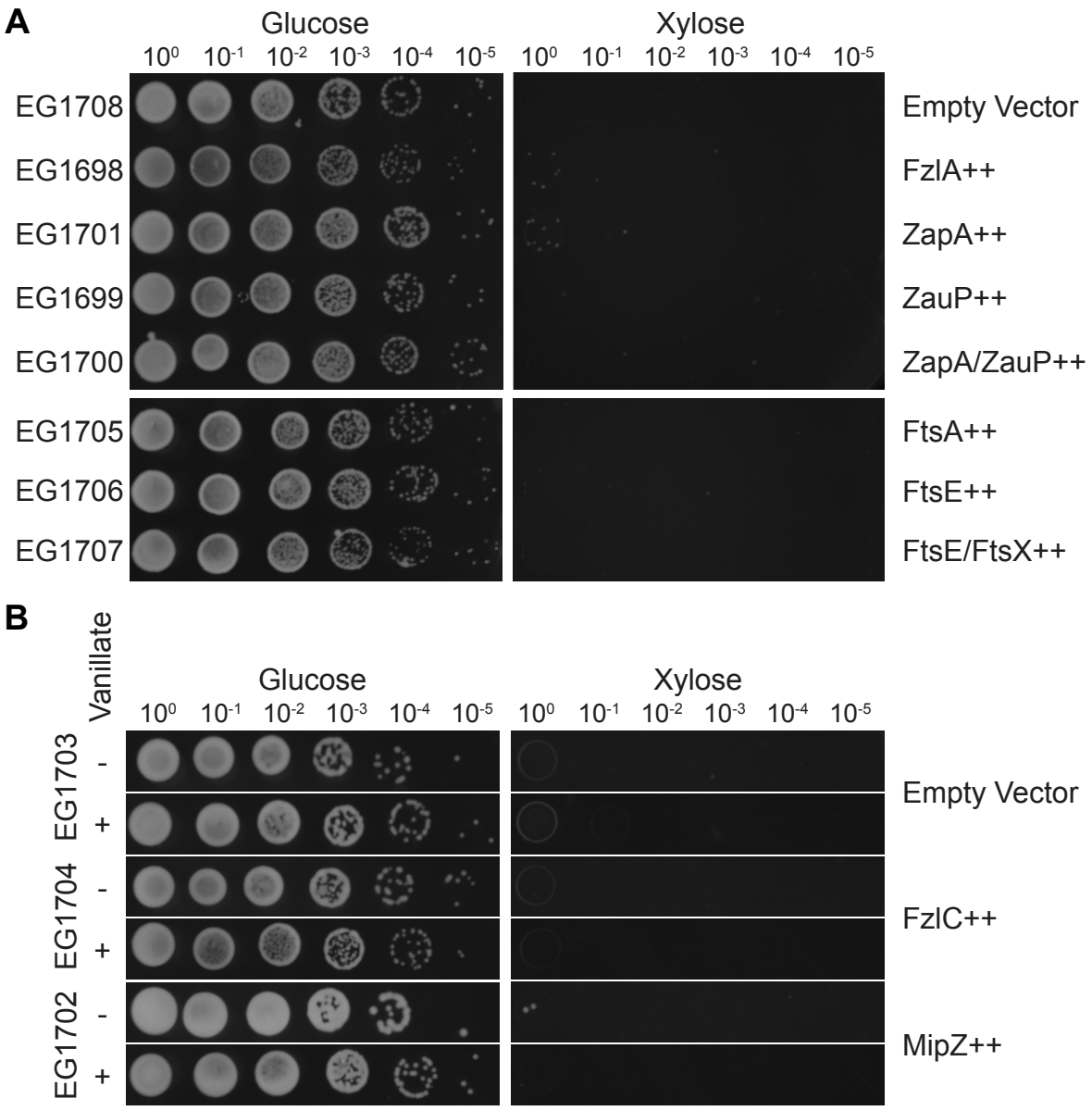
A
Glucose
Xylose
10^0 10^-1 10^-2 10^-3 10^-4 10^-5
EG1708
EG1698
EG1701
EG1699
EG1700
EG1705
EG1706
EG1707
Empty Vector
FzlA++
ZapA++
ZauP++
ZapA/ZauP++
FtsA++
FtsE++
FtsE/FtsX++
B
Vanillate
EG1703
EG1704
EG1702
-
+
Empty Vector
FzlC++
MipZ++

Figure S9

Figure S9: Overexpression of FtsZ binding partners does not suppress ΔCTL-induced growth defects.

A.-B. Spot dilutions of strains in Figure 3 showing growth of cells uninduced (glucose) or induced (xylose) for Δ*CTL* expression. Cells in log phase were diluted to an OD_{600} of 0.05, serially diluted, and spotted onto PYE agar plates with indicated inducer (glucose, xylose, and/or vanillate). Plates were incubated at 30˚C for 48 hours before imaging. Strain key (all have xylose-inducible Δ*CTL*): Empty Vector (EG1708), FzlA++ (EG1698), ZapA++ (EG1701), ZauP++ (EG1699), ZapA/ZauP++ (EG1700), FtsA++ (EG1705), FtsE++ (EG1706), FtsE/FtsX++ (EG1707), Empty Vector (EG1703), FzlC++ (EG1704), MipZ++ (EG1702)

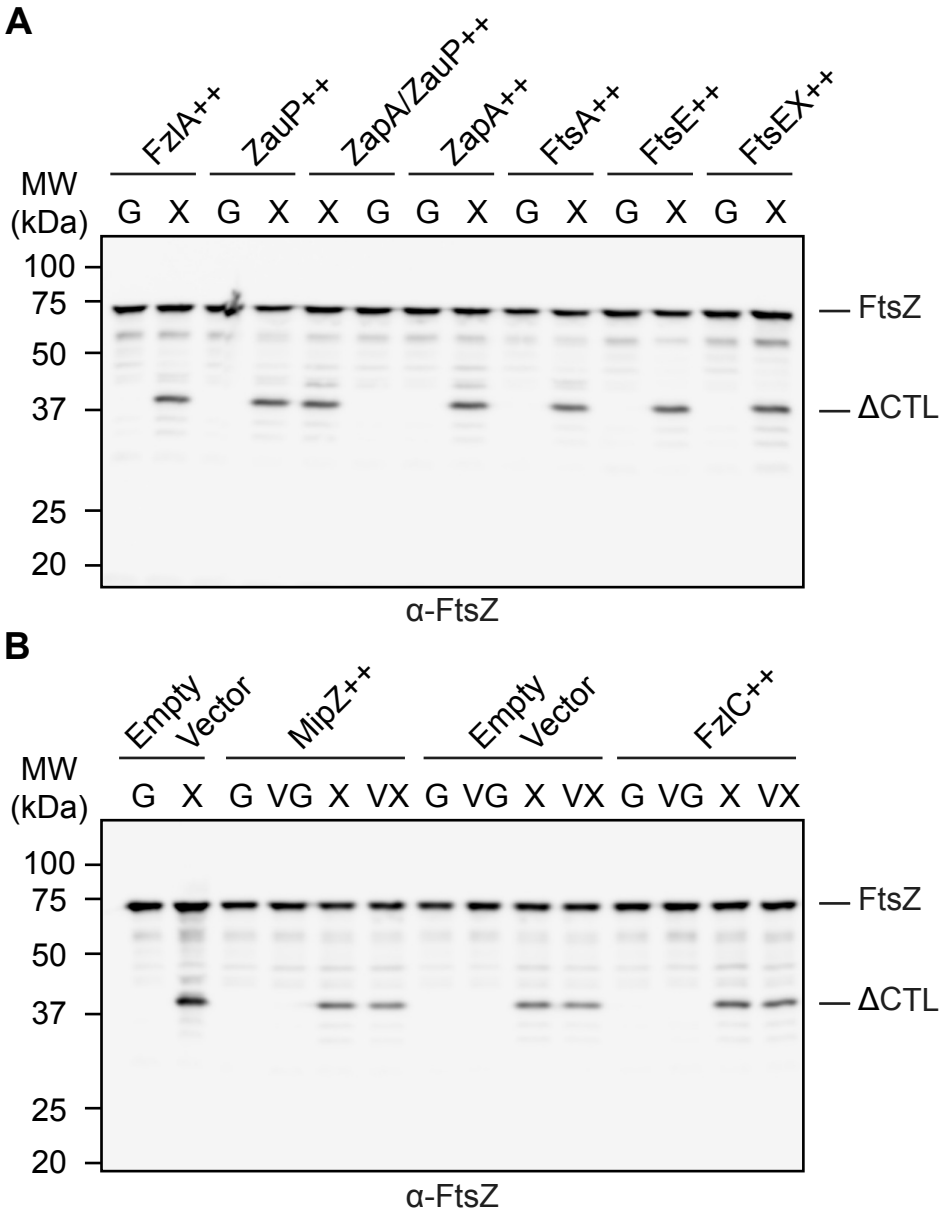
A
FzlA++
ZauP++
ZapA/ZauP++
ZapA++
FtsA++
FtsE++
FtsEX++
MW (kDa)
G X G X X G G X G X G X G X
100
75
50
37
25
20
— FtsZ
— ΔCTL
α-FtsZ
B
Empty Vector
MipZ++
Empty Vector
FzlC++
MW (kDa)
G X G VG X VX G VG X VX G VG X VX
100
75
50
37
25
20
— FtsZ
— ΔCTL
α-FtsZ

Figure S10

Figure S10: Levels of FtsZ and ΔCTL are not impacted by overexpression of binding partners.

A.-B. Immunoblots using anti-FtsZ antibody showing protein levels of ΔCTL and WT FtsZ corresponding to the experiments in Figure 3 at 6.5 hours of incubation with inducers (glucose or G, vanillate or V, xylose or X). Strain key (all have xylose-inducible Δ*CTL*): Empty Vector (EG1708), FzlA++ (EG1698), ZapA++ (EG1701), ZauP++ (EG1699), ZapA/ZauP++ (EG1700), FtsA++ (EG1705), FtsE++ (EG1706), FtsE/FtsX++ (EG1707), Empty Vector (EG1703), FzlC++ (EG1704), MipZ++ (EG1702)

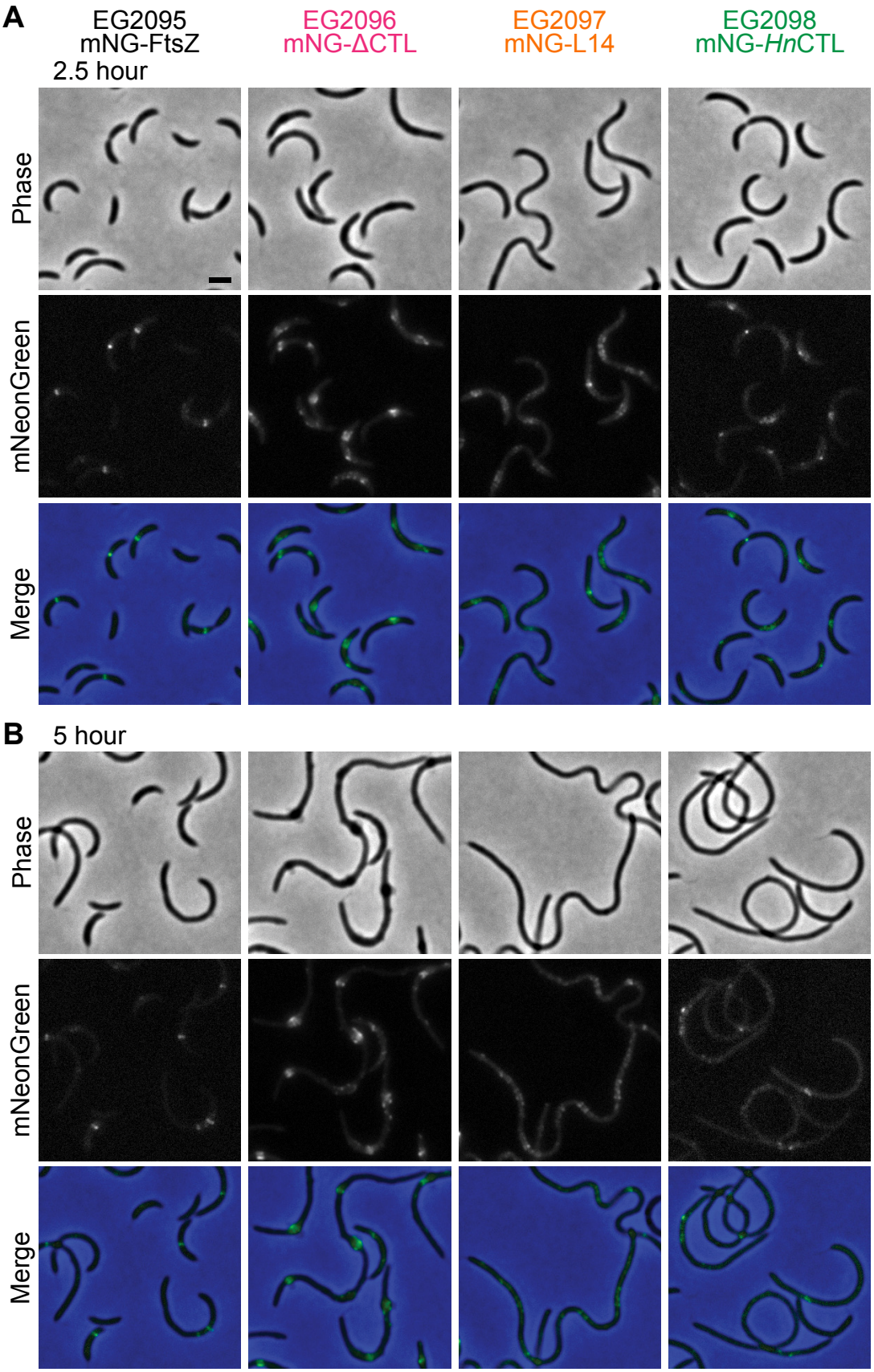
A
EG2095
mNG-FtsZ
EG2096
mNG-ΔCTL
EG2097
mNG-L14
EG2098
mNG-*Hn*CTL
2.5 hour
Phase
mNeonGreen
Merge
B
5 hour
Phase
mNeonGreen
Merge

Figure S11

Figure S11: ΔCTL assembles into large asymmetric superstructures at sites of cell wall bulging in cells depleted of WT FtsZ.

A.-B. Phase contrast, epifluorescence, and merged images of cells induced with xylose to drive expression of *mNG-FtsZ, mNG-ΔCTL, mNG-L14,* or *mNG*-Hn*CTL* from P_{xylX} promoter for 2.5 hours (**A**) or 5 hours (**B**) while simultaneously depleting WT FtsZ. Scale bar – 2 μm. Strain key: mNG-FtsZ (EG2095), mNG-ΔCTL (EG2096), mNG-L14 (EG2097), mNG-*Hn*CTL (EG2098)

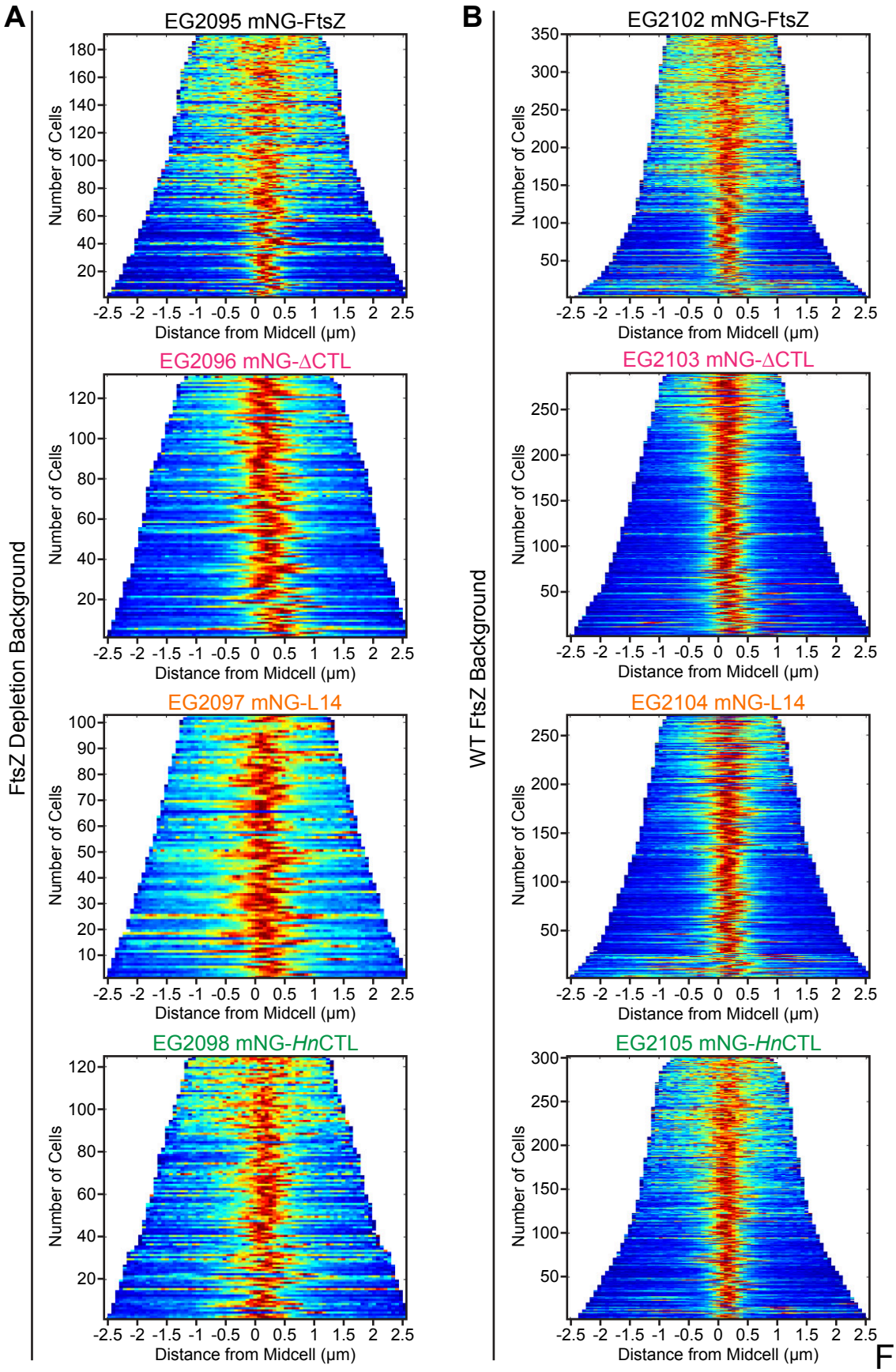
A
FtsZ Depletion Background
EG2095 mNG-FtsZ
EG2096 mNG-ΔCTL
EG2097 mNG-L14
EG2098 mNG-HnCTL
B
WT FtsZ Background
EG2102 mNG-FtsZ
EG2103 mNG-ΔCTL
EG2104 mNG-L14
EG2105 mNG-HnCTL
Number of Cells
Distance from Midcell (μm)

Figure S12

Figure S12: Demographs show differences in FtsZ distribution among CTL variants in FtsZ depletion and FtsZ WT backgrounds.

A.-B. Demographs showing mNG intensity as a function of cell length (blue = least intense pixel in each cell, red = most intense pixel in each cell) of a population of cells (length ≤ 5 μm) represented in Figure 5A (**A**) and Figure S14A (**B**). Strain key: mNG-FtsZ (EG2095), mNG-ΔCTL (EG2096), mNG-L14 (EG2097), mNG-*Hn*CTL (EG2098), mNG-FtsZ/FtsZ (EG2102), mNG-ΔCTL/FtsZ (EG2103), mNG-L14/FtsZ (EG2104), mNG-*Hn*CTL/FtsZ (EG2105)

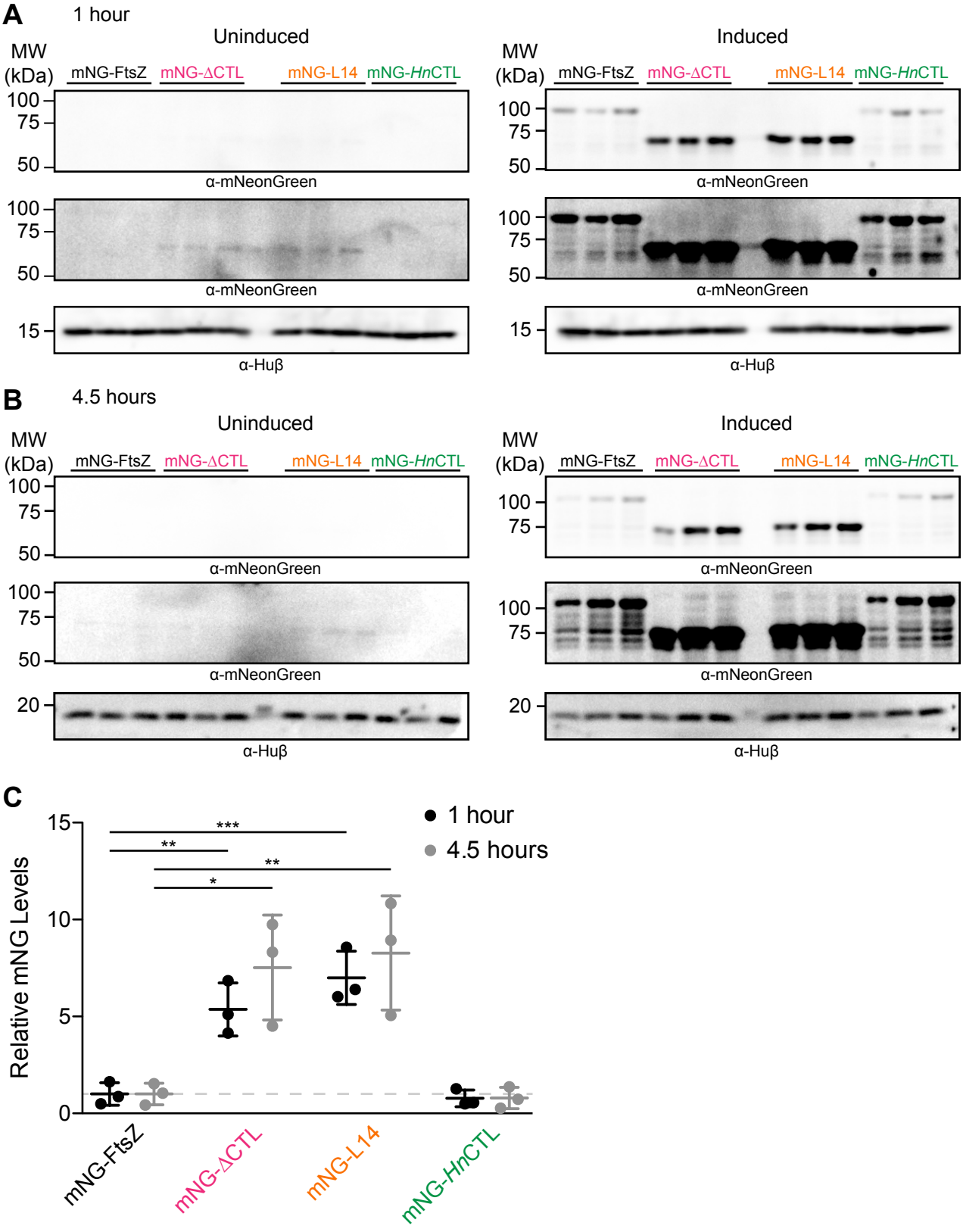
A
1 hour
Uninduced
Induced
MW (kDa)
mNG-FtsZ
mNG-ΔCTL
mNG-L14
mNG-HnCTL
100
75
50
15
α-mNeonGreen
α-Huβ
B
4.5 hours
20
C
1 hour
4.5 hours
Relative mNG Levels
0
5
10
15
***
**
**
*

Figure S13

Figure S13: mNG-ΔCTL and mNG-L14 FtsZ variants are present at elevated levels in cells depleted for WT FtsZ.

A.-B. Immunoblots using anti-mNeonGreen antibody against lysates from cells depleted for FtsZ and uninduced (glucose and vanillate) or induced (xylose) for *mNG-FtsZ, mNG-*Δ*CTL, mNG-L14,* or *mNG*-Hn*CTL* for 1 hour (**A**) or 4.5 hours (**B**). Overexposed blots are also shown below each blot to validate lack of signal in uninduced controls. Anti-Huβ antibody was used as concentration control for loading and quantification. **C.** Quantification of immunoblots from A. and B. showing relative abundance of mNG-FtsZ variants after 1 hour (black) or 4.5 hours (grey). Bars represent standard deviation. * - $P \leq 0.05$; ** - $P \leq 0.01$; *** - $P \leq 0.001$. Strain key: mNG-FtsZ (EG2095), mNG-ΔCTL (EG2096), mNG-L14 (EG2097), mNG-*Hn*CTL (EG2098)

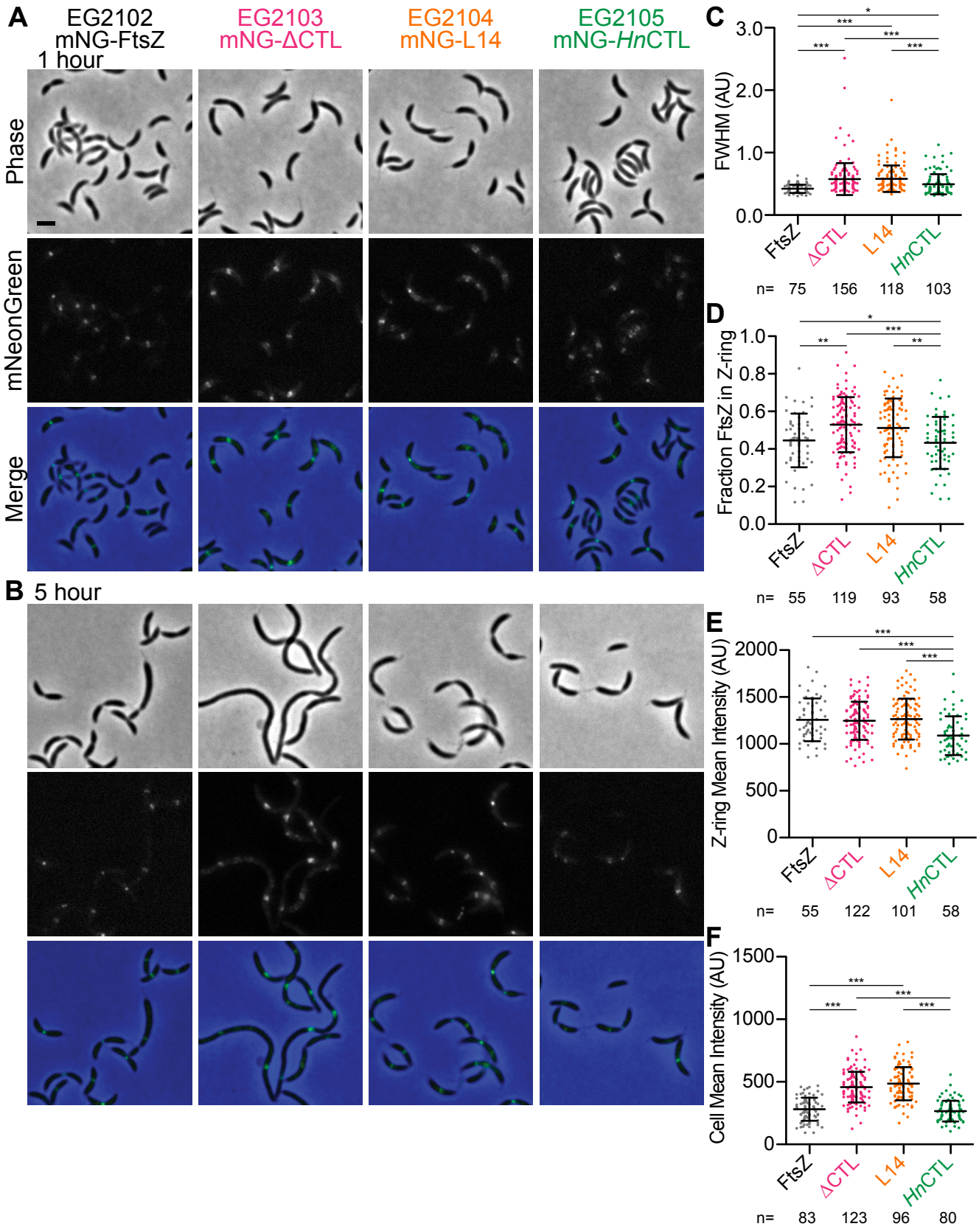
A
EG2102
mNG-FtsZ
EG2103
mNG-ΔCTL
EG2104
mNG-L14
EG2105
mNG-HnCTL
1 hour
Phase
mNeonGreen
Merge
B
5 hour
C
FWHM (AU)
3.0
2.0
1.0
0.0
FtsZ
ΔCTL
L14
HnCTL
n= 75 156 118 103
D
Fraction FtsZ in Z-ring
1.0
0.8
0.6
0.4
0.2
0.0
n= 55 119 93 58
E
Z-ring Mean Intensity (AU)
2000
1500
1000
500
0
n= 55 122 101 58
F
Cell Mean Intensity (AU)
1500
1000
500
0
n= 83 123 96 80

Figure S14

Figure S14: The CTL impacts Z-ring organization in the presence of WT FtsZ.

A.-B. Phase contrast, epifluorescence, and merged images of cells induced with xylose to drive expression of *mNG-FtsZ, mNG-*Δ*CTL, mNG-L14,* or *mNG*-Hn*CTL* from P_{xylX} promoter for 1 hour (**A**) or 5 hours (**B**) in strains producing WT FtsZ. **C.-F.** Quantification of epifluorescence images of cells 3 to 5 μm long indicating the full-width at half max (FWHM) values of Z-ring intensity (**C**)**,** fraction of mNG-FtsZ or variants in the Z-ring (**D**), and mean epifluorescence intensity of the whole cells (**E**) or the Z-ring (**F**) in a WT FtsZ background. Bars represent standard deviation. * - $P \leq 0.05$; ** - $P \leq 0.01$; *** - $P \leq 0.001$. Numbers of cells per strain are indicated for each measurement. Strain key: mNG-FtsZ/FtsZ (EG2102), mNG-ΔCTL/FtsZ (EG2103), mNG-L14/FtsZ (EG2104), mNG-*Hn*CTL/FtsZ (EG2105)

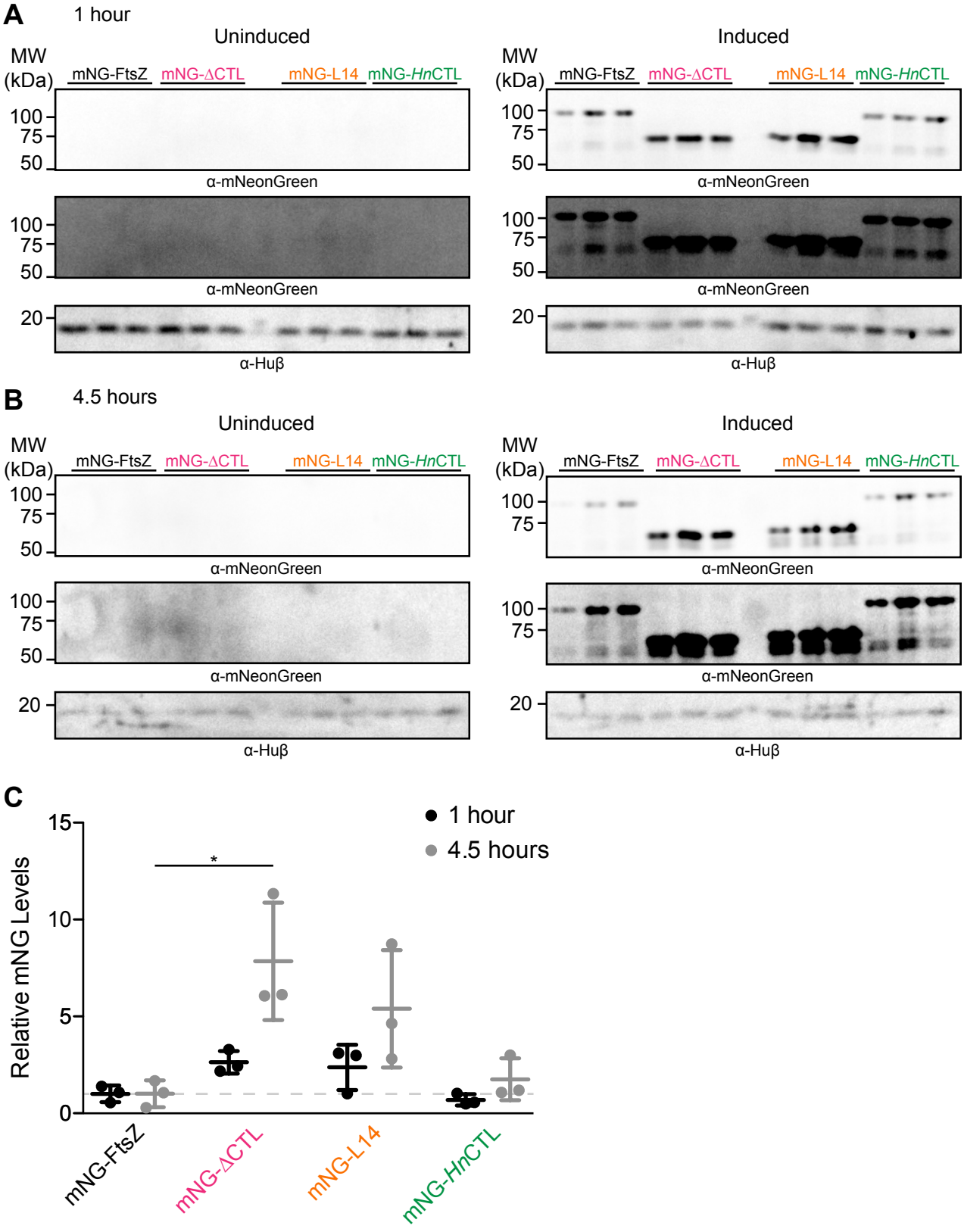
A
1 hour
Uninduced
Induced
MW (kDa)
mNG-FtsZ
mNG-ΔCTL
mNG-L14
mNG-HnCTL
100
75
50
20
α-mNeonGreen
α-Huβ
B
4.5 hours
C
1 hour
4.5 hours
Relative mNG Levels
15
10
5
0
*

Figure S15

Figure S15: mNG-ΔCTL FtsZ is present at elevated levels in the presence of WT FtsZ.

A.-B. Immunoblots using anti-mNeonGreen antibody against lysates from cells uninduced (glucose) or induced (xylose) for *mNG-FtsZ, mNG-*Δ*CTL, mNG-L14,* or *mNG-*Hn*CTL* for 1 hour (**A**) or 4.5 hours (**B**). Overexposed blots are also shown below each blot to validate lack of signal in uninduced controls. Anti-Huβ antibody was used as concentration control for loading and quantification. **C.** Quantification of immunoblots from A. and B. showing relative abundance of mNG-FtsZ variants after 1 hour (black) or 4.5 hours (grey). Bars represent standard deviation. * - $P \leq 0.05$. Strain key: mNG-FtsZ/FtsZ (EG2102), mNG-ΔCTL/FtsZ (EG2103), mNG-L14/FtsZ (EG2104), mNG-*Hn*CTL/FtsZ (EG2105)

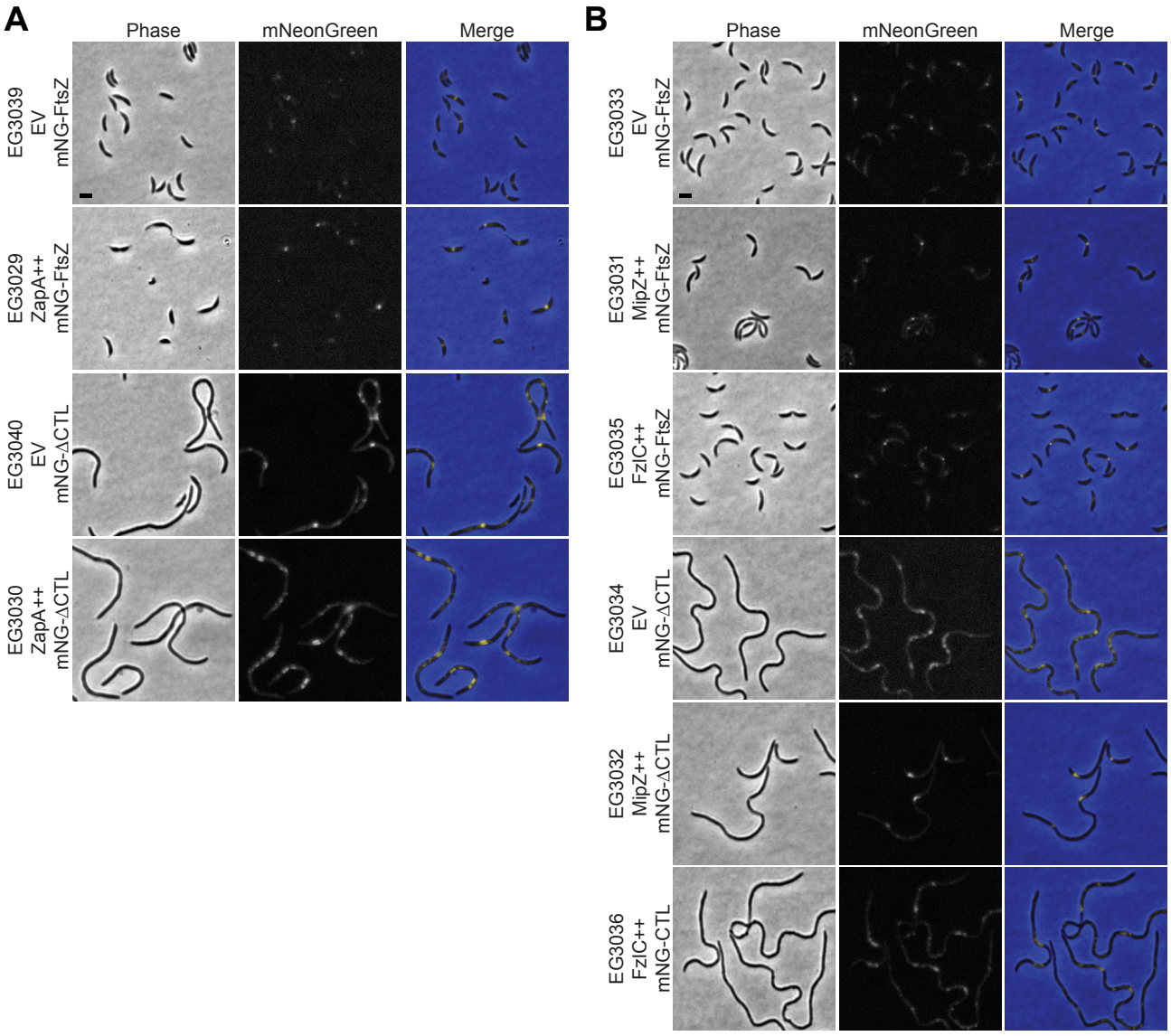
A
Phase
mNeonGreen
Merge
EG3039 EV mNG-FtsZ
EG3029 ZapA++ mNG-FtsZ
EG3040 EV mNG-ΔCTL
EG3030 ZapA++ mNG-ΔCTL
B
Phase
mNeonGreen
Merge
EG3033 EV mNG-FtsZ
EG3031 MipZ++ mNG-FtsZ
EG3035 FzlC++ mNG-FtsZ
EG3034 EV mNG-ΔCTL
EG3032 MipZ++ mNG-ΔCTL
EG3036 FzlC++ mNG-CTL

Figure S16

Figure S16: mNG-FtsZ and mNG-ΔCTL localization are unaffected by overproduction of ZapA, MipZ, or FzlC.

A. Phase contrast, epifluorescence, and merged images of cells induced with xylose to drive expression of either *mNG-FtsZ* or *mNG-ΔCTL* and empty vector or *zapA* from P_{xylX} promoter for 6.5 hours. **B.** Phase contrast, epifluorescence, and merged images of cells induced with xylose and vanillate to drive expression of either *mNG-FtsZ* or *mNG-ΔCTL* from P_{xylX} and empty vector, *mipZ*, or *fzlC* from P_{vanA} promoter for 6.5 hours. Scale bar – 2 μm. Strain key: Empty vector/mNG-FtsZ (EG3039), ZapA++/mNG-FtsZ (EG3029), Empty vector/mNG-ΔCTL (EG 3040), ZapA++/mNG-ΔCTL (EG3030), Empty vector/mNG-FtsZ (EG3033), MipZ++/mNG-FtsZ (EG3031); FzlC++/mNG-FtsZ (EG3035); Empty vector/mNG-ΔCTL (EG3034), MipZ++/mNG-ΔCTL (EG3032), FzlC++/mNG-ΔCTL (EG3036)

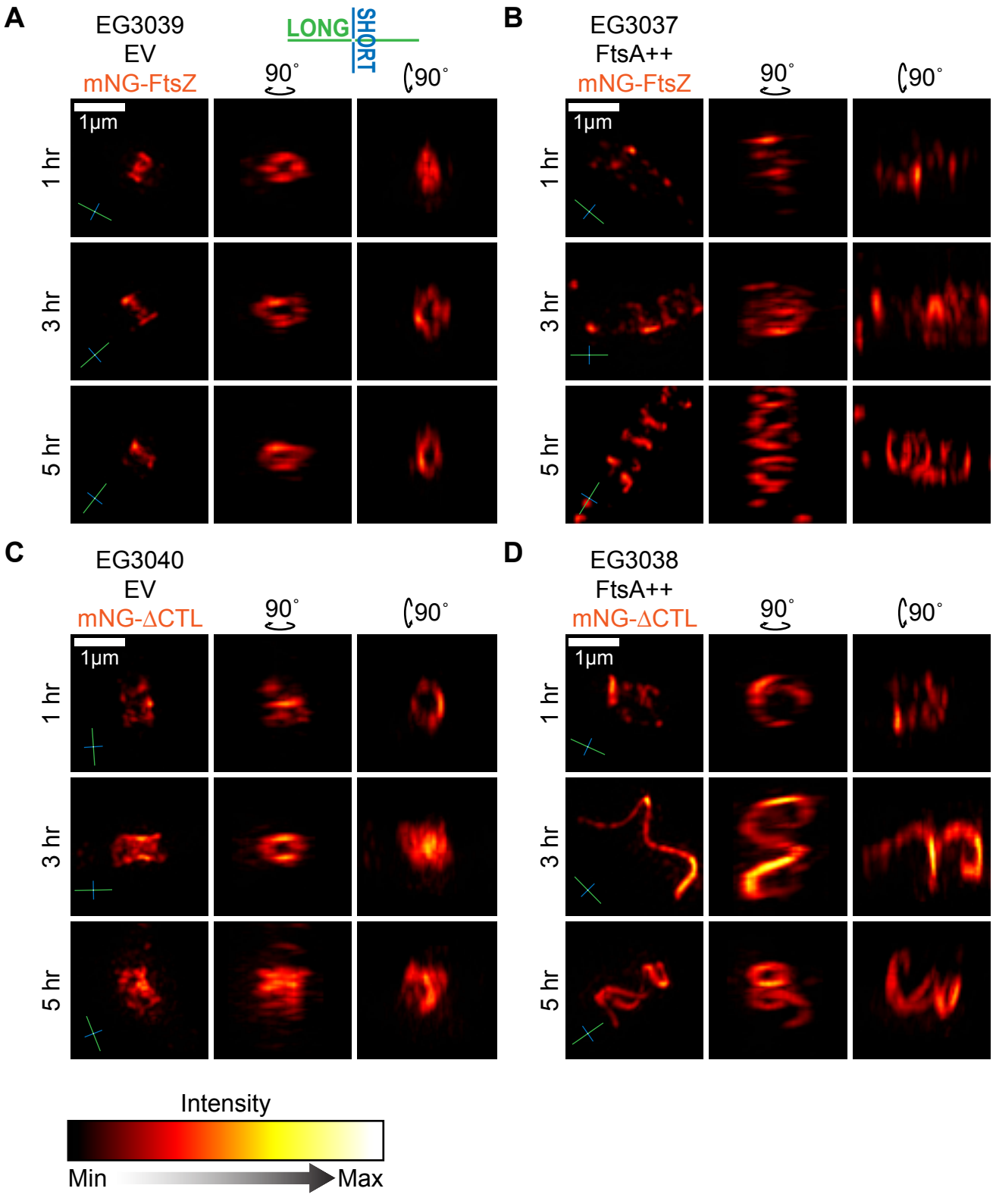
A
EG3039
EV
mNG-FtsZ
LONG
SHORT
90˚
90˚
1μm
1 hr
3 hr
5 hr
B
EG3037
FtsA++
mNG-FtsZ
90˚
90˚
1μm
1 hr
3 hr
5 hr
C
EG3040
EV
mNG-ΔCTL
90˚
90˚
1μm
1 hr
3 hr
5 hr
D
EG3038
FtsA++
mNG-ΔCTL
90˚
90˚
1μm
1 hr
3 hr
5 hr
Intensity
Min
Max

Figure S17

Figure S17: FtsA overproduction interferes with Z-ring assembly and causes mNG-ΔCTL to form long helical structures *in vivo*

A.-D. Orthogonal views of 3D-projections of image stacks acquired by 3D-SIM visualization of Z-rings in cells induced with xylose to drive expression of empty vector and *mNG-FtsZ* (**A**), *ftsA* and *mNG-FtsZ* (**B**), empty vector and *mNG-*Δ*CTL* (**C**), or *ftsA* and *mNG-*Δ*CTL* (**D**) from P_{xylX} promotor for indicated amounts of time. Compasses in lower left of each image indicate the orientation of long (green) and short (blue) axes of cells. Scale bars – 1 μm. Strain key: Empty vector/mNG-FtsZ (EG3039), FtsA++/mNG-FtsZ (EG3037), Empty vector/mNG-ΔCTL (EG3040), FtsA++/mNG-ΔCTL (EG3038)

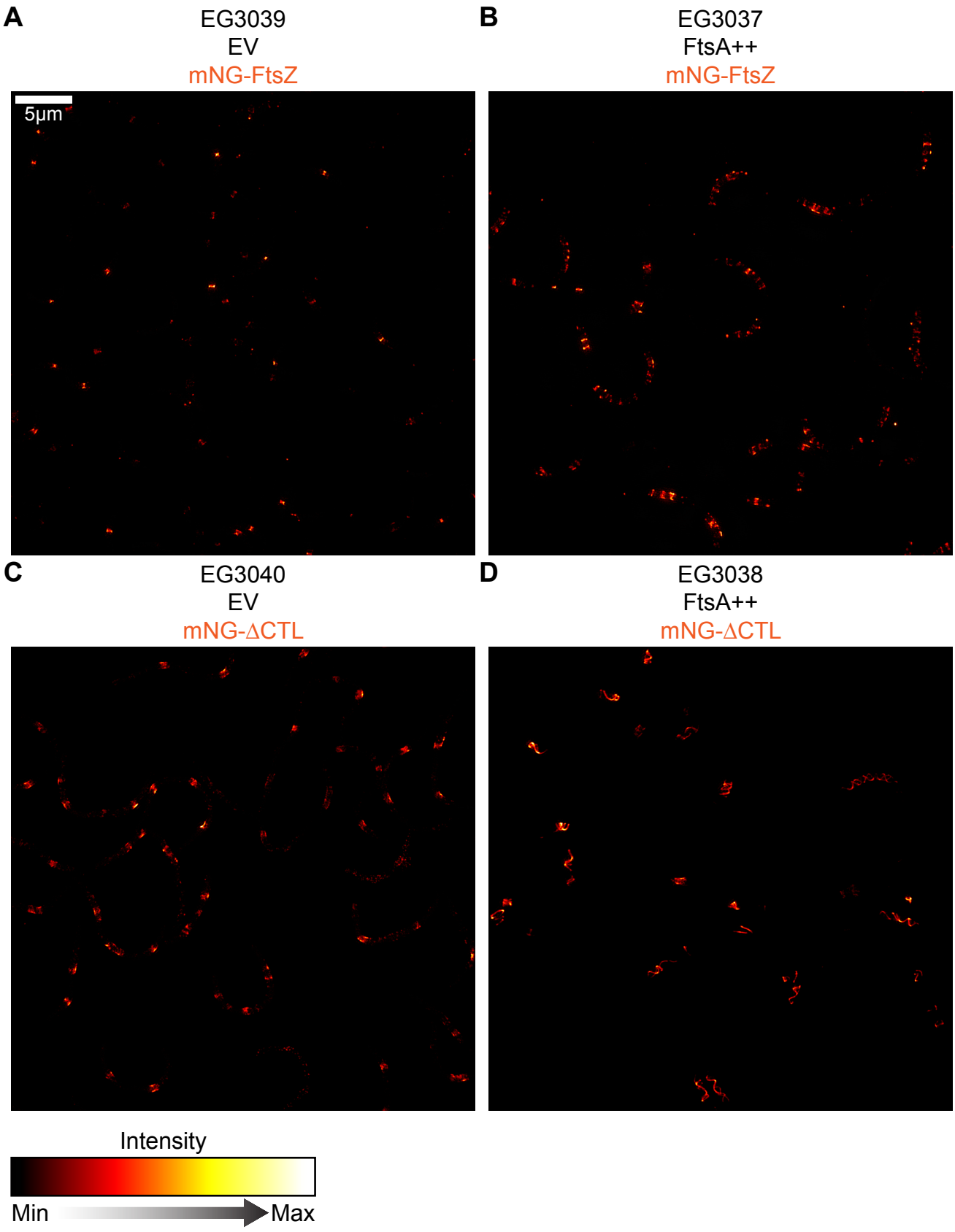
A
EG3039
EV
mNG-FtsZ
5μm
B
EG3037
FtsA++
mNG-FtsZ
C
EG3040
EV
mNG-ΔCTL
D
EG3038
FtsA++
mNG-ΔCTL
Intensity
Min
Max

Figure S18

Figure S18: Representative 3D-SIM z-projections showing mNG-FtsZ and mNG-ΔCTL Z-ring morphologies.

A.-D. Three dimensional z-projections generated from whole field of view image stacks acquired by 3D-SIM visualization of Z-rings in cells induced with xylose to drive expression of empty vector and *mNG-FtsZ* (**A**), *ftsA* and *mNG-FtsZ* (**B**), empty vector and *mNG-*Δ*CTL* (**C**), or *ftsA* and *mNG-*Δ*CTL* (**D**) from P_{xylX} promotor for 5 hours prior to imaging. Scale bar – 5 μm. Strain key: Empty vector/mNG-FtsZ (EG3039), FtsA++/mNG-FtsZ (EG3037), Empty vector/mNG-ΔCTL (EG3040), FtsA++/mNG-ΔCTL (EG3038)

Supplemental Videos S1-4: Movies of 3D-SIM mNG-FtsZ or mNG-ΔCTL Z-ring morphologies

Movies showing wobble representations of three-dimensional z-projections generated from fields of view from image stacks acquired by 3D-SIM visualization of cells induced with xylose to drive expression of *mNG-FtsZ* and empty vector (**1**), *mNG-FtsZ* and *ftsA* (**2**), *mNG-*Δ*CTL* and empty vector (**3**), or *mNG-*Δ*CTL* and *ftsA* (**4**) from P_{xylX} promotor for 5 hours prior to imaging. Scale bar – 1 μm. Strain key: Empty vector/mNG-FtsZ (EG3039), FtsA++/mNG-FtsZ (EG3037), Empty vector/mNG-ΔCTL (EG3040), FtsA++/mNG-ΔCTL (EG3038)

Supplemental Table S1: List of strains used in this study

Supplemental Table S2: List of plasmids used in this study